Available online at www.sciencedirect.com
SCIENCE DIRECT®
Tetrahedron 60 (2004) 979–986
Tetrahedron

A new series of heteroaromatic receptors containing the 1,3-bis(6-oxopyridazin-1-yl)propane unit: their selective transport ability towards NH_4^+ in relation to Na^+, K^+ and Ca^{2+}

Lucrecia Campayo,[a] Mercedes Pardo,[a,*] Ana Cotillas,[a] Oscar Jaúregui,[a] Maria J. R. Yunta,[a] Carmen Cano,[a] Fernando Gomez-Contreras,[a] Pilar Navarro[b] and Ana M. Sanz[a]

[a]*Departamento de Quimica Organica I, Facultad de Quimica, Universidad Complutense, 28040 Madrid, Spain*
[b]*Instituto de Quimica Medica, C.S.I.C., Juan de la Cierva, 3, 28006 Madrid, Spain*

Received 23 July 2003; revised 21 October 2003; accepted 12 November 2003

Abstract—The synthesis of a new series of heteroaromatic macrocycles **6**–**9** containing the 1,3-bis(6-oxopyridazin-1-yl)propane and pyridine units is reported. The acyclic compounds **11**–**15** had to be prepared as the intermediates in the synthetic sequence. Evaluation of the ionophoric properties of **6**–**9** and **11**–**15** shows that **8** and **13** behave as good ammonium ion carriers and exhibit a high selectivity for ammonium with respect to spherically symmetric metallic ions like Na^+, K^+, and Ca^{2+}. Molecular modelling of the ammonium complexes suggests that the host's oxyimino groups play a more relevant part in effective complexation than the pyridine unit, and that the high complexating efficiency of **13** might be related to the formation of a pseudocavity by intramolecular hydrogen bonding.

1. Introduction

In the last decades, a considerable interest has been shown in developing selective receptors for the ammonium cation.[1] Such receptors can be used as NH_4^+ sensors in clinical analysis, environmental chemistry, and many other applications.[2] One of the most effective NH_4^+ receptors is nonactin,[3] the natural antibiotic agent commercially used in ion-selective electrodes.[4] However, a serious drawback of nonactin is that it binds only about ten times more tightly to NH_4^+ than to K^+. Similarly, crown ethers show little or no selectivity for binding NH_4^+ against K^+,[3] although the substitution of oxygen atoms by nitrogen increases ammonium selectivity,[5] and pyrido crown ethers have shown to be specially effective in NH_4^+/K^+ discrimination.[6] Achieving selectivity in the complexation of ammonium in relation to metal ions of biological importance like Na^+, K^+ or Ca^{2+} is a significative goal because it could allow some kind of control in transporting the above cations across biological membranes.

Our group has been involved for years in the study of the ionophoric properties of mono- and dinuclear receptors containing sp^2 nitrogen heterocyclic units. We have demonstrated that 36-membered dinuclear ether and ester crowns of 3,5-disubstituted 1*H*-pyrazole containing tetraethyleneglycol units, **1** (Fig. 1), are able to facilitate the NH_4^+ transport, but lack the desired NH_4^+/K^+ selectivity.[7] The introduction of pyridine rings in the flexible oxygenated chains of **1** to give **2** provided better ammonium selectivity by cooperation of the sp^2 heterocyclic nitrogen atoms when they could be included into the macrocyclic cavity.[8] On the other hand, when the macrocyclic ring size was reduced to 26 atoms by linking the heterocyclic moieties with diethyleneglycol units (**3**–**4**), the NH_4^+ complexation ability was improved, because of a better cooperativity of the pyrazole sp^2 nitrogens.[9,10] Subsequently, we introduced the 1,3-bis(1*H*-pyrazol-1-yl)propane unit in the macrocyclic ring, as exemplified in **5**. All the heteroatoms in these compounds have the electron lone pairs oriented inside the cavity, and the propylenic fragment should favour conformational mobility for accommodation of the guest. However, selectivity for the ammonium ion was less than that one obtained in the previous series.[11]

With the aim of improving the ionophoric properties found for **5** and analogues, we have prepared here a new family of heteroaromatic receptors (**6**–**9**). The conformational mobility provided by the 1,3-propylene fragment in **5** has been maintained, and the cooperative effects of the pyrazolic nitrogens substituted by those of two pyridazinone units. The presence of a pyridine ring both modifies the macrocyclic ring flexibility and contributes to a more

Keywords: Heteroaromatic receptors; Ammonium carriers; Pyridazine macrocycles.
* Corresponding author. Tel.: +34-913944230; fax: +34-913944103; e-mail address: merpar@quim.ucm.es

0040–4020/$ - see front matter © 2003 Elsevier Ltd. All rights reserved.
doi:10.1016/j.tet.2003.11.040

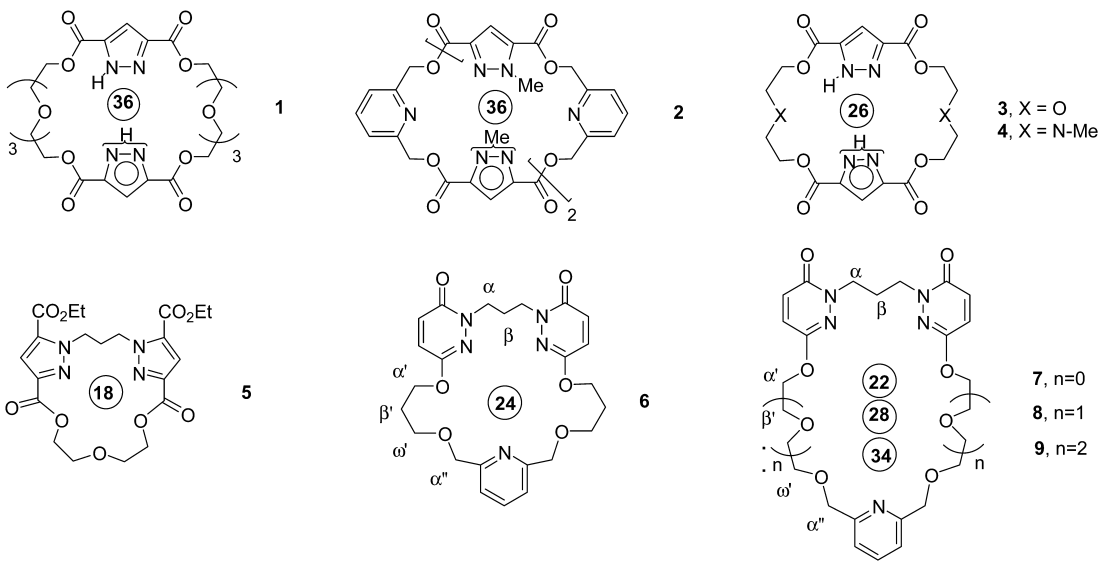

Figure 1.

effective complexation through the sp^2 heterocyclic nitrogen, as shown previously for **2**.[8] The respective presence of ethyleneoxy or propyleneoxy units modifies the relative distance between the pyridazine ring and the oxyimino fragments, as presumed main sites for ammonium complexation. The ionophoric properties of compounds **6**–**9** and their open chain precursors in the synthetic process have been evaluated against NH_4^+ and the biologically significative Na^+, K^+, and Ca^{2+} cations.

2. Results and discussion

We have used 1,3-bis(3-chloro-6-oxopyridazin-1-yl)-propane, **10**, as the synthon for the preparation of both the acyclic and cyclic receptors. This compound was in turn obtained from 3,6-dichloropyridazine via the mono-potassium salt of 3-chloro-6(1*H*)-pyridazinone[12] as shown in Scheme 1, in a whole yield of 67%. A side product in the last step is the mono-O-alkylation compound, that must be separated and is formed in 17% yield.

First, the *O*-butyl substituted derivative **11** was prepared in order to set the reaction conditions. It could be formed in a 48% yield by the reaction of **10** with the alkoxide generated in situ from butanol, that was also the solvent, using a stoichiometric 4:1 sodium excess. Following the same procedure, the acyclic compounds **12** and **13**–**15** were synthesized by treatment of the synthon **10** with 1,3-propanediol or polyethyleneglycol units of different lenghts, in yields between 41 and 57%.

In turn, the cyclic derivatives **6** and **7**–**9** were obtained by heating the previously formed diols with 2,6-bis(bromo-methyl)pyridine in the presence of sodium hydride in a dimethoxyethane–dimethylformamide solution at 60 °C.

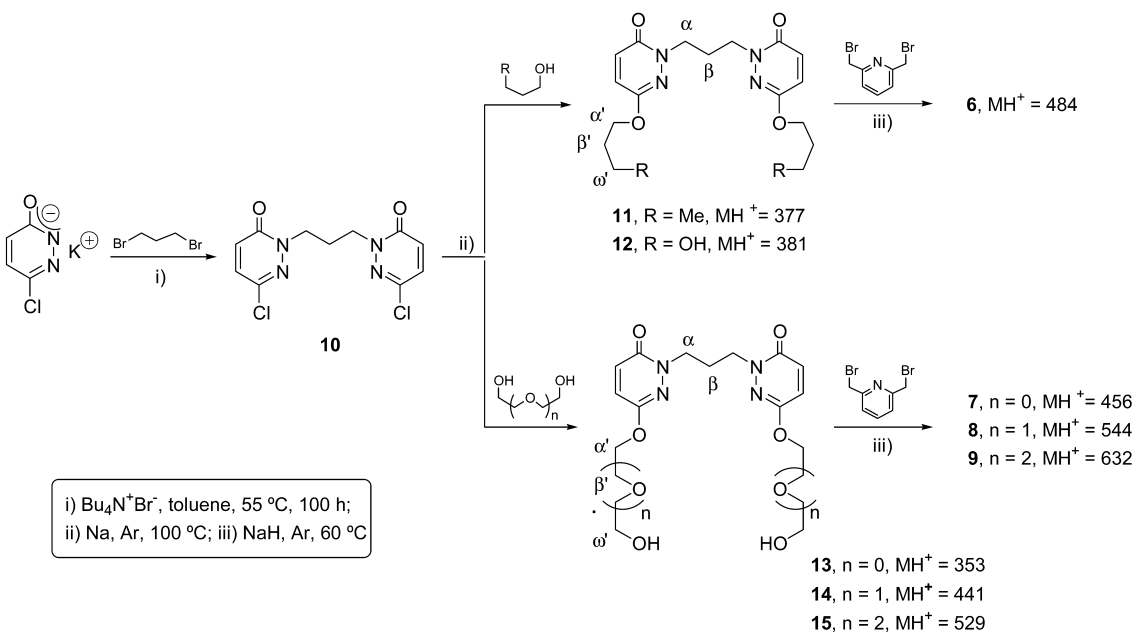

Scheme 1.

Both the cyclic and acyclic receptors were purified by flash column chromatograpy and usually isolated as stable crystalline solids.

Structures were assigned on the basis of analytical, and spectroscopic mass, IR, and ^{1}H and ^{13}C NMR data. Molecular ions obtained from FAB mass spectra fit the proposed structures and agree in most cases with the base peak (see Scheme 1).

The ^{1}H NMR pyridazinone signals are easily differentiated from those of the pyridine ring, appearing as neat AB systems with coupling constants in the range of 9.6–9.9 Hz. Concerning the aliphatic moieties, Tables 1 and 2 show the ^{1}H and ^{13}C values for signals corresponding to the methylene groups. In all cases, those vicinal to the pyridazine nitrogens are more shielded in the ^{1}H spectra than their counterparts neighbouring the oxyimino groups. Furthermore, both types of methylenes can be differentiated by the shape of the corresponding signals, which are shown as neat triplets coupled to quintuplets in the α units, whereas the α′ ones display variable multiplicities and J values. In the ^{13}C spectra, the CH_2–N signals appear in the vicinity of 50 ppm, but the CH_2–oxyimino are substantially more deshielded (around 65 ppm).

On the other hand, if we compare compounds containing ethylenic and propylenic chains, the methylene groups of **7**–**9** and **13**–**15** are seen in the ^{1}H spectra as the typical multiplet pairs in the AA′BB′ system of the –O–CH_2–CH_2–O– units.[13] However, in **6** and **12** the CH_2 vicinal to oxymino group are always shown as triplets.

As expected, the methylenic hydrogens in the ω′ position of the acyclic derivatives are more shielded than the rest, and in the ^{13}C spectra the CH_2–OH carbons also seem to be the most shielded among those vicinal to oxygen. The protons at the methylene groups vicinal to the pyridine ring appear in the cyclic compounds as sharp singlets between 4.5 and 4.7 ppm, and their carbons are the most deshielded among all the aliphatic ones.

All compounds reported in this paper have been evaluated as carriers of Na^+, K^+, Ca^{2+}, and NH_4^+ picrates in passive transport processes using a classical bulk liquid membrane of chloroform as indicated in Section 3.[11] Picrate anions have been selected on the basis of their lipophilic character and also because they are surface active, favouring the transfer of the cations from the aqueous phase to the interface.[14]

Table 2. ^{13}C NMR [CD_3OD, δ (ppm)] chemical shifts of the most significative methylene carbons in compounds **6**–**9** and their acyclic precursors **12**–**15**

	C_α	C_β	$C_{\alpha'}$	$C_{\beta'}$	$C_{\omega'}$	$C_{\alpha''}$
6	49.84	27.86	65.56	30.12	68.19	74.54
12	50.01	27.27	65.36	32.67	59.36	—
7	49.48	27.56	66.75	—	69.22	73.78
13	49.49	25.93	69.60	—	60.82	—
8	50.88	26.24	67.93	70.17	71.77	75.17
14	50.06	27.41	68.06	70.33	62.51	—
9	52.55	26.95	68.00	70.36	71.70	74.63
15	50.11	27.41	67.96	70.17	62.51	—

The resulting transport rates are gathered in Table 3. It can be observed that, in accordance with our initial design, all the new series of cyclic compounds **6**–**9** transport NH_4^+ better than Na^+, K^+, and Ca^{2+}. In fact, the cyclic receptor **8** in which the two heteroaromatic units are linked by diethylene glycol flexible chains behaves as the most effective carrier of ammonium ions (ν=57 μM h^{-1}). Furthermore, this ligand exhibits an excellent selectivity for NH_4^+ in relation to the three metallic cations evaluated (NH_4^+/Na^+=9.2, NH_4^+/K^+=9.5, NH_4^+/Ca^{2+}=11.8).

It is interesting to point out that the size of the macrocyclic cavity seems to be critical in order to achieve both efficiency and selectivity in the ammonium transport. Taking as the reference the cavity size of **8** (28-membered), it can be observed that smaller or larger cavities lead to both lower transport rates and selectivities. Thus, compounds with 24 (**6**) and 22 (**7**) members are almost five times less effective carriers that **8**, and compound **9** (34-membered) is the worst carrier in this cyclic series.

In relation to the evaluation of the ionophoric properties in the acyclic intermediates **11**–**15**, it is shown that all of them are unable to efficiently transport Na^+, K^+, and Ca^{2+} ions. However, the acyclic intermediate **13**, in which the 1,3-bis(6-oxopyridazin-1-yl)propane unit has been functionalized with shorter flexible chains of ethylene glycol, behaves as an efficient carrier of NH_4^+ ions. Furthermore, compound **13** displays an excellent selectivity of NH_4^+ transport in relation to K^+(NH_4^+/K^+=73), which is almost seven times higher than that one of nonactin.[2] Finally, an impressive selectivity in relation to Ca^{2+}(NH_4^+/Ca^{2+}=146) is also observed. This fact could be related to the hydration grade of the cation inside the complex, as it is dependant of the cation charge.[15]

It is interesting to note that the hydroxy groups of **13**,

Table 1. ^{1}H NMR [CD_3OD, δ (ppm)] chemical shifts of the most significative methylene protons in compounds **6**–**9** and their acyclic precursors **12**–**15**

	H_α	H_β	$H_{\alpha'}$	$H_{\beta'}$	$H_{\omega'}$	$H_{\alpha''}$
6	4.06 (t, 4H)[a]	2.33 (q, 2H)[a]	4.21 (t, 4H)[b]	2.12 (q, 4H)[b]	3.71 (t, 4H)[b]	4.54 (s, 4H)
12	4.03 (t, 4H)[a]	2.24 (q, 2H)[a]	4.16 (t, 4H)[b]	1.87 (q, 4H)[b]	3.61 (t, 4H)[b]	—
7	3.90 (t, 4H)[a]	2.08 (q, 2H)[a]	4.38 (m, 4H)	—	3.84 (m, 4H)	4.63 (s, 4H)
13	4.11 (t, 4H)[a]	2.32 (q, 2H)[a]	4.22 (m, 4H)	—	3.84 (m, 4H)	—
8	4.11 (t, 4H)[a]	2.33 (q, 2H)[a]	4.38 (m, 4H)		3.6–3.8 (m, 4H)	4.67 (s, 4H)
14	4.12 (t, 4H)[a]	2.34 (q, 2H)[a]	4.31 (m, 4H)	3.82 (m, 4H)	3.61 (m, 4H)	—
9	4.10 (t, 4H)[a]	2.32 (q, 2H)[a]	4.23 (m, 4H)	3.89 (m, 4H)	3.71 (m, 4H)	4.61 (s, 4H)
15	4.12 (t, 4H)[a]	2.33 (q, 2H)[a]	4.31 (m, 4H)	3.82 (m, 4H)	3.6–3.8 (m, 4H)	—

[a] J=6.9 Hz.
[b] J=6.3 Hz.

Table 3. Transport rates ($\times\mu M\,h^{-1}$) of alkali, alkaline earth, and ammonium ions through a chloroform phase containing 7×10^{-4} M of cyclic **6**–**9** and acyclic **11**–**15** carriers

	Transport rates				Selectivity		
	Na^+	K^+	Ca^{2+}	NH_4^+	NH_4^+/Na^+	NH_4^+/K^+	NH_4^+/Ca^{2+}
6	4.9	2.6	1.3	11.8	2.4	4.1	9.1
7	2.0	3.8	2.2	10.1	5.0	2.6	4.6
8	6.3	6.9	4.9	**57.9**	**9.2**	**9.5**	**11.8**
9	3.3	4.5	2.0	5.2	1.6	1.1	2.6
11	1.8	0.8	1.7	1.5	0.8	1.8	0.9
12	0.5	1.8	1.7	0.1	0.2	0.05	0.14
13	0.7	0.8	0.4	**58.4**	**83.4**	**73.0**	**146.0**
14	0.6	0.6	0.8	0.1	0.16	0.16	0.13
15	0.5	4.2	0.3	0.7	1.4	0.16	2.3

located at a shorter distance from the heteroaromatic moiety, seem to play a critical role in the complexation process of ammonium, since the butoxy substituted derivative **11** and the hydroxy substituted compounds **12**, **14** and **15** are worse carriers of this ion.

In order to evaluate the possible ammonium-receptor interactions involved in the complexes formed by the most promising carriers found in this work, we have performed molecular modelling of the NH_4^+ complexes formed from ligands **8** and **13**. With the aim of justifying the transport differences observed with the rest of the cyclic series, the complex of the 24-membered compound **6**, which exhibits a macrocyclic cavity relatable to that one of **8** was also included in the modelling studies. The additive AMBER force field has been used because it is specially adequate for describing the complexation processes of our ligands, since it is the best method[16] for reproducing H-bonding and stacking stabilization energies. Methodology and conventions used are summarized in Section 3.

Figures 2 and 3 display the most stable conformations obtained for the cyclic receptor 1:1 complexes **6**-NH_4^+ and

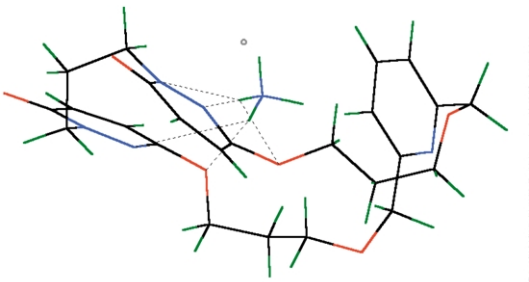

E_c = -15.30 Kcal/mol

NH····N(2)-Pdz A; NH····N(2)-Pdz B; NH·····N(1)-Pdz B
NH·····O-C_3(Pdz A); NH·····O-C_3 (Pdz B)

Figure 3. Molecular modelling, complexation energy, and hydrogen bonding in **6**.

8-NH_4^+. Intermolecular hydrogen bondings between the ligand's heteroatoms and the ammonium ion are also shown, together with the lowest complexation energies found in every case. In **8**, the 28-membered macrocycle has the two pyridazinone rings oriented in a parallel way and has a bowl-shaped conformation around the ammonium ion, that is located outside the macrocyclic cavity in a suitable disposition for allowing simultaneous effective interaction with the nitrogen atoms at the three heterocyclic rings and the oxygens at the aliphtic chains. Therefore, one of the ammonium hydrogens interacts in a trifurcated way with the imine nitrogens of the two pyridazine rings, the second ammonium hydrogen is linked to the nitrogen at the pyridine ring and to one of the oxygens nearest to pyridine. Finally, the other two are bonded to the central oxygens at the aliphatic chains and to the oxyimine oxygen neighbouring one of the pyridazine units.

In contrast, the most favoured conformation obtained for the ammonium complex of the smaller 24-membered macrocycle **6** (Fig. 3) implies a more planar disposition of the macrocyclic ring with divergent pyridazine rings, and the ammonium ion is mainly interacting with the oxygen and

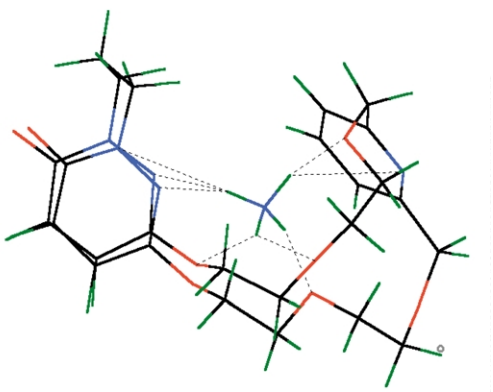

E_c = -21.98 Kcal/mol

NH····N(2)-PdzA; NH····N(2)-Pdz B; NH·····N(1)-Pdz B;
NH·····N-Pyr; NH·····O-CH_2 Pyr.
NH·····O-C_3(Pdz A); NH·····O-$CH_{2\,\beta',\,\gamma'}$
NH·····O-$CH_{2\,\beta',\,\gamma'}$

Figure 2. Molecular modelling, complexation energy, and hydrogen bonding in **8**.

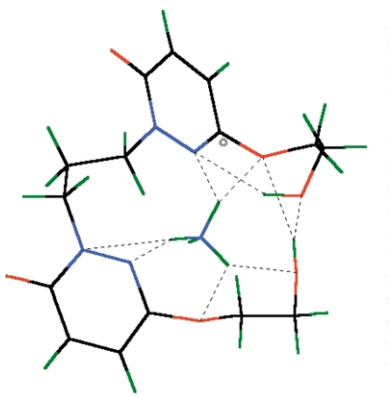

E_c = -15.19 Kcal/mol

NH·····N(2)-Pdz A; NH·····N(1)-Pdz A
NH·····N(2)-Pdz B; NH·····O-C_3 (Pdz B)
NH·····O-C_3 (Pdz A); NH·····OH
OH·····O-C_3 Pdz B; OH·····OH; OH····· N(2)-Pdz B

Figure 4. Molecular modelling, complexation energy, and hydrogen bonding in **13**.

nitrogen atoms at the oxyimino groups. As a consequence, the calculated complexation energy is substantially lower in absolute value than that one found for **8** (ΔE_c=6.68 kcal/mol). All this suggests that both the size of the macrocyclic cavity and the participation of the flexible chains oxygens might be decisive in order to achieve an effective transport.

The most favoured conformation for the ammonium complex of the effective acyclic carrier **13** is shown in Figure 4. This complex exhibits strong intramolecular bonding between the terminal OH groups forming a pseudomacrocyclic structure that wraps the guest. On the other hand, the ammonium hydrogens give way to intermolecular interactions with the imine nitrogens at the pyridazine rings, and also with the oxygen atoms at the oxyimino groups. All this is reflected in a complexation energy of −15.90 kcal/mol. The high transport efficiency found for this ligand with respect to the other acyclic compounds tested could be due to its smaller size, that allows the formation of a pseudocavity favouring closeness of the ammonium hydrogens and the oxyimino moieties and giving place to a more effective interaction. Molecular modelling of ligands **12**, **14**, and **15** leads always to bigger pseudocavities and less favourable complexation energies than those calculated for **13**.

Finally, if we compare the complexation energies obtained for **8** and **13**, it should be noted that, although both compounds exhibit similar transport efficiency for the ammonium ion, complexation seems to be clearly more favoured in **8** with respect to **13**. However, it is well known[17] that complexation/decomplexation processes have a great influence on transport rates, and that they are usually much more favoured in acyclic carriers than in cyclic ones.[18]

3. Experimental

3.1. General

Reagents were purchased from commercial suppliers and used without further purification, unless otherwise stated. Ligands were prepared in dry solvents under an argon atmosphere. Reaction courses were routinely monitored by TLC on precoated aluminium sheets of silica gel, and compounds were detected with UV light (245 nm) and/or iodine chamber. Chromatographic separations were performed on columns, using the flash chromatography technique on silica gel (particle size 0.040–0.063 mesh) and as eluent a mixture of toluene/ethyl acetate/methanol/dichloromethane (1:2:1:1, v:v), unless otherwise indicated. Melting points were measured in open capillaries and are uncorrected. The ^{1}H NMR spectra were recorded at 300 MHz and the ^{13}C NMR spectra were recorded at 75 or 100 MHz at room temperature in the solvent indicated in each case. Chemical shifts are given as δ values, using TMS as internal standard, and coupling constants are given in Hz. Mass spectra were recorded by the fast atomic bombardment (FAB) technique using a *m*-nitrobenzyl alcohol matrix. 3-Chloro-1*H*-pyridazin-6-one was obtained following a previously described procedure starting from 3,6-dichloropyridazine.[12]

3.1.1. 1,3-Bis(3-chloro-6-oxopyridazin-1-yl)propane (10). A mixture of the potassium salt of 3-chloro-1*H*-pyridazin-6-one (prepared by reaction with a equimolecular amount of potassium hydroxide in ethanol) (2.28 g, 13 mmol), 1,3-dibromopropane (1.40 g, 7 mmol), and tetrabutylammonium chloride (1.08 g, 3 mmol) in anhydrous toluene (65 mL) was heated at 65 °C for 100 h. After cooling to room temperature, the residual solid was filtered and the solution was evaporated to dryness under reduced pressure. The residue was purified by column chromatography (toluene/ethyl acetate/ethanol, 2:1:0.15). The most retained fraction afforded 3.09 g (67% yield) of **10** as a yellow solid. Mp 124–5 °C. IR (KBr, cm^{-1}) 3040, 1680 (C=O), 1590; ^{1}H NMR ($CDCl_3$) δ 7.18 (d, J=10 Hz, 2H), 6.91 (d, J=10 Hz, 2H), 4.20 (t, J=7 Hz, 4H), 2.33 (q, J=7 Hz, 2H); ^{13}C NMR ($CDCl_3$) δ 158.88, 137.53, 133.61, 132.02, 49.13, 26.84. Anal. calcd for $C_{11}H_{10}N_4O_2Cl_2$: C, 43.87; H, 3.35; N, 18.60; Cl, 23.54. Found: C, 44.10; H, 3.58; N, 18.69; Cl, 23.03.

3.2. General procedure for the synthesis of podands 11–15

To a solution of 4–5 mmol of sodium in excess of the appropriate alcohol or glycol 1 mmol of dichloroderivative **10** was added. The mixture was heated to 100 °C for 1 h, diluted with 10 mL of water when cold, and extracted with chloroform. Solvent and excess of glycol was removed under reduced pressure and the crude product was purified by chromatography on silica gel.

3.2.1. 1,3-Bis(3-butoxy-6-oxopyridazin-1-yl)propane (11). Following the general procedure, flash chromatography on silica gel of the residue obtained in the reaction of **10** (0.5 mmol) with 1-butanol (4 mL) and sodium (2.5 mmol) afforded 90 mg (48%) of a pure oil identified as **11**. (R_f=0.33, toluene/ethyl acetate/ethanol, 2:1:0.15). IR ($CHCl_3$, cm^{-1}) 1685 (C=O), 1595, 1225; ^{1}H NMR (CD_3OD) δ 7.09 (d, J=9.6 Hz, 2H); 6.91 (d, J=9.6 Hz, 2H), 4.17 (t, J=7.2 Hz, 4H), 4.12 (t, J=6.6 Hz, 4H), 2.32 (q, J=6.6 Hz, 2H), 1.73 (m,4H), 1.47 (m, 4H), 0.98 (t, J=7.5 Hz, 6H); ^{13}C NMR (CD_3OD) δ 161.28, 155.31, 133.65, 128.85, 68.48, 49.99, 32.13, 27.62, 20.54, 14.56. MS (FAB, *m/z*) 377 (MH^+, 100); HRMS (FAB) calcd for $[MH]^+$ $C_{19}H_{29}N_4O_4$ 377.2188, obsd. 377.2194.

3.2.2. 1,3-Bis[3-(3-hydroxypropoxy)-6-oxopyridazin-1-yl)propane (12). Chromatography on silica gel of the residue obtained in the reaction of **10** (300 mg, 1 mmol) with sodium (100 mg, 4.34 mmol) in 5 mL of 1,3-propanediol afforded 150 mg (41%) of **12** as a white solid (R_f=0.35). Mp 137–8 °C. IR (KBr, cm^{-1}), 3380 (O–H), 1660 (C=O), 1585, 1300; ^{1}H NMR (CD_3OD) δ 7.02 (d, J=9.6 Hz, 2H), 6.82 (d, J=9.6 Hz, 2H), 4.16 (t, J=6.3 Hz, 4H), 4.03 (t, J=6.9 Hz, 4H), 3.61 (t, J=6.3 Hz, 4H), 2.24 (q, J=6.9 Hz, 2H); 1.87 (q, J=6.3 Hz, 4H); ^{13}C NMR (CD_3OD) δ 161.01, 154.96, 133.35, 128.54, 65.36, 59.36, 50.01, 32.67, 27.27. MS (FAB, *m/z*) 381 (MH^+, 32); 136 (100). Anal. calcd for $C_{17}H_{24}N_4O_6$: C, 53.59; H, 6.30; N, 14.71. Found: C, 53.63; H, 6.27; N, 14.35.

3.2.3. 1,3-Bis[3-(2-hydroxyethoxy)-6-oxopyridazin-1-yl)propane (13). Chromatography on silica gel of the residue obtained in the reaction of **10** (500 mg, 1.66 mmol) with sodium (100 mg, 4.34 mmol) in 4 mL of ethylene glycol afforded 244 mg (42%) of **13** (R_f=0.33). Mp 162–4 °C. IR (KBr, cm^{-1}) 1665 (C=O), 1590, 1300; ^1H NMR (CD_3OD) δ 7.14 (d, J=9.6 Hz, 2H), 6.93 (d, J=9.6 Hz, 2H), 4.22 (m, 4H), 4.11 (t, J=6.9 Hz, 4H), 3.84 (m, 4H), 2.32 (q, J=6.9 Hz, 2H); ^{13}C NMR (CD_3OD) δ 160.89, 154.74, 133.33, 128.42, 69.60, 60.82, 49.50, 27.47. MS (FAB, *m/z*) 353 (MH^+, 100). Anal. calcd for $C_{15}H_{20}N_4O_6 \cdot 1/2H_2O$: C, 49.86; H, 5.86; N, 15.50. Found: C, 49.95; H, 5.56; N, 15.21.

3.2.4. 1,3-Bis{3-[2-(2-hydroxyethoxy)ethoxy]-6-oxopyridazin-1-yl}propane (14). Chromatography on silica gel of the residue obtained in the reaction of **10** (300 mg, 1 mmol) with sodium (100 mg, 4.34 mmol) in 5 mL of diethylene glycol afforded 180 mg (41%) of **14** as a white solid (R_f=0.34). Mp 103–4 °C. IR (KBr, cm^{-1}) 3140 (O–H), 1670 (C=O), 1590, 1300; ^1H NMR (CD_3OD) δ 7.13 (d, J=9.6 Hz, 2H), 6.94 (d, J=9.6 Hz, 2H), 4.31 (m, 4H); 4.12 (t, J=6.9 Hz, 4H), 3.82 (m, 4H), 3.68 (m, 4H), 3.61 (m, 4H), 2.34 (q, J=6.9 Hz, 2H); ^{13}C NMR (CD_3OD) δ 161.31, 155.04, 133.83, 128.80, 74.06, 70.33, 68.06, 62.50, 50.06, 27.41. MS (FAB, *m/z*) 441 (MH^+, 100). Anal. calcd for $C_{19}H_{28}N_4O_8 \cdot 1/2H_2O$: C, 50.77; H, 6.50; N, 12.47. Found: C, 50.99; H, 6.24; N, 12.53.

3.2.5. 1,3-Bis(3-{2-[2-(2-hydroxyethoxy)ethoxy]ethoxy}-6-oxopyridazin-1-yl)propane (15). Chromatography on silica gel of the residue obtained in the reaction of **10** (300 mg, 1 mmol) with sodium (100 mg, 4.34 mmol) in 5 mL of triethylene glycol afforded 300 mg (57%) of **15** as a colorless oil (R_f=0.34). IR (KBr, cm^{-1}) 3140 (O–H), 1670 (C=O), 1590, 1300; ^1H NMR (CD_3OD) δ 7.13 (d, J=9.6 Hz, 2H), 6.94 (d, J=9.6 Hz, 2H), 4.31 (m, 4H), 4.12 (t, J=6.9 Hz, 4H), 3.82 (m, 4H), 3.67 (m, 12H), 3.58 (m, 4H), 2.33 (q, J=6.9 Hz, 2H). ^{13}C NMR (CD_3OD) δ 161.34, 155.03, 133.87, 128.83, 74.01, 71.99, 71.72, 70.41, 67.96, 62.51, 50.11, 27.41. MS (FAB, *m/z*) 529 (MH^+, 100). Anal. calcd for $C_{23}H_{36}N_4O_{10}$: C, 52.27; H, 6.82; N, 10.61. Found: C, 52.07; H, 6.91; N, 10.54.

3.2.6. 10,14,22,26-Tetraoxa-1,5,31,32,33-pentaazatetracyclo[25.3.1.1^{5,9}.1^{16,20}]tritriaconta-7,9(32),16,18,20(33),27(31),28-heptaen-6,30-dione (6). To a solution of diol **12** (60 mg, 0.16 mmol) in THF (30 mL), potassium *tert*-butoxide (56 mg, 0.5 mmol) was added and the reaction mixture was kept at 60 °C until the salt of **12** was formed (0.5 h). Then, a solution of 2,6-bis(bromomethyl)pyridine (43 mg, 0.16 mmol) in THF (10 mL) was added slowly. After the addition was complete, the reaction mixture was kept for 4 h at 60 °C, then cooled to room temperature, and stirred overnight. The resulting reaction mixture was filtered, evaporated to dryness, and the residue was chromatographed on silica gel. Fractions of R_f=0.45 afforded 14 mg (18%) of crown **6** as a pure colorless oil. ^1H NMR (CD_3OD) δ 7.78 (t, J=7.8 Hz, 1H), 7.38 (d, J=7.8 Hz, 2H), 7.10 (d, J=9.6 Hz, 2H), 6.92 (d, J=9.6 Hz, 2H), 4.54 (s, 4H), 4.21 (t, J=6.9 Hz, 4H), 4.06 (t, J=6.9 Hz, 4H), 3.71 (t, J=6.0 Hz, 4H); 2.33 (q, J=6.0 Hz, 2H), 2.15 (q, J=6.9 Hz, 4H); ^{13}C NMR (CD_3OD) δ 160.93, 158.78, 154.89, 139.01, 133.35, 128.51, 123.26, 74.54, 68.19, 65.56, 49.84, 30.12, 27.86. MS (FAB, *m/z*) 484 (MH^+, 90); HRMS (FAB) calcd for $[MH]^+$ $C_{24}H_{30}N_5O_6$ 484.219609, obsd. 484.218100.

3.2.7. 10,13,21,24-Tetraoxa-1,5,29,30,31-pentaazatetracyclo[23.3.1.1^{5,9}.1^{15,19}]untriaconta-7,9(30),15,17,19(31),25(29),26-heptaen-6,28-dione (7). To a stirred suspension of NaH (93 mg, 3.88 mmol) in DME (30 mL) a solution of diol **13** (352 mg, 1 mmol) in a mixture of DMF (8 mL) and DME (40 mL) was added and the reaction was kept at 60 °C until the disodium salt of **13** was formed (0.5 h). Then, the mixture was diluted with 100 mL of DME and, after the temperature was again stabilized at 60 °C, a solution of 2,6-bis(bromomethyl)pyridine (265 mg, 1 mmol) in DME (100 mL) was added over a period of 2–3 h. After the addition was completed, the reaction was kept for 4 h at 60 °C, then cooled to room temperature, and stirred overnight. Further treatment with water, filtration, and extraction with dichloromethane afforded and organic layer that was evaporated to dryness and the residue column chromatographed on silica gel. Fractions of R_f=0.36 afforded 57 mg (13%) of crown **7** as a white solid. Mp 174–6 °C. ^1H NMR (CD_3OD) δ 7.63 (t, J=7.8 Hz, 1H), 7.23 (d, J=7.8 Hz, 2H), 7.16 (d, J=9.9 Hz, 2H), 6.95 (d, J=9.9 Hz, 2H), 4.63 (s, 4H), 4.38 (m, 4H), 3.90 (t, J=6.9 Hz, 4H), 3.84 (m, 4H), 2.08 (q, J=6.9 Hz, 2H); ^{13}C NMR (CD_3OD) δ 160.83, 159.06, 154.63, 138.85, 133.52, 128.71, 122.36, 73.78, 69.22, 66.75, 49.48, 27.58. MS (FAB, *m/z*) 456 (MH^+, 100); HRMS (FAB) calcd for [MH^+] $C_{22}H_{26}N_5O_6$ 456.188309, obsd. 456.189090.

3.2.8. 10,13,16,24,27,30-Hexaoxa-1,5,35,36,37-pentaazatetracyclo[29.3.1.1^{5,9}.1^{18,22}]heptatriaconta-7,9(36),18,20,22(37),31(35),32-heptaen-6,34-dione (8). To a stirred suspension of NaH (56 mg, 2.35 mmol) in DME (50 mL) was added a solution of diol **14** (517 mg, 1.18 mmol) in a mixture of DMF (3 mL) and DME (30 mL), and the reaction mixture was kept at 60 °C until the disodium salt of **14** was formed (0.5 h). Then, the mixture was diluted with 70 mL of DME and potassium carbonate (81 mg, 0.59 mmol) was added. After the temperature was again stabilized at 60 °C, a solution of 2,6-bis(bromomethyl)pyridine (312 mg, 1.18 mmol) in DME (100 mL) was added over a period of 2–3 h. After the addition was complete, the reaction mixture was kept for 4 h at 60 °C, then cooled to room temperature, and stirred overnight. The resulting reaction mixture was treated with water, filtered, and extracted with chlorophorm. The organic extracts were evaporated to dryness and the residue was chromatographed on silica gel. Fractions of R_f=0.42 afforded 32 mg (5%) of crown **8** as a solid. Mp 104–6 °C. ^1H NMR (CD_3OD) δ 7.72 (t, J=7.8 Hz, 1H), 7.39 (d, J=7.8 Hz, 2H), 7.00 (d, J=9.6 Hz, 2H), 6.91 (d, J=9.6 Hz, 2H); 4.67 (s, 4H), 4.18 (m, 4H), 4.11 (t, J=6.6 Hz, 4H); 3.79–3.73 (m, 12H), 2.33 (q, J=6.6 Hz, 2H). ^{13}C NMR (CD_3OD) δ 161.29, 159.62, 154.79, 139.19, 133.93, 128.79, 121.98, 75.17, 72.78, 71.71, 70.17; 67.93, 50.88, 26.24. MS (FAB, *m/z*) 544 (MH^+, 100); HRMS (FAB) calcd for [MH^+] $C_{26}H_{34}N_5O_8$ 544.240739, obsd. 544.241300.

3.2.9. 10,13,16,19,27,30,33,36-Octaoxa-1,5,41,42,43-pentaazatetracyclo[35.3.1.1^{5,9}.1^{21,25}]tritetraconta-7,9(42),

18,20,22(37),31(35),32-heptaen-6,34-dione (9). To a stirred suspension of NaH (96 mg, 4 mmol) in DME (50 mL) was added a solution of diol **15** (1056 mg, 2 mmol) in DME (50 mL), and the reaction mixture was kept at 60 °C until the disodium salt of **15** was formed (0.5 h). Then, the mixture was diluted with 200 mL of DME and cesium chloride (337 mg, 2 mmol) was added. After the temperature was again stabilized at 60 °C, a solution of 2,6-bis(bromomethyl)pyridine (530 mg, 2 mmol) in DME (200 mL) was added over a period of 2–3 h. After the addition was complete, the reaction mixture was kept for 4 h at 60 °C, then cooled to room temperature, and stirred overnight. The resulting reaction mixture was treated with water, filtered, and extracted with chlorophorm. The organic extracts were evaporated to dryness and the residue was chromatographed on silica gel. Fractions of R_f=0.42 afforded 170 mg (27%) of crown **9** as an oil. ^{1}H NMR (CD_3OD) δ 7.73 (t, J=7.8 Hz, 1H), 7.41 (d, J=7.8 Hz, 2H), 6.99 (d, J=9.6 Hz, 2H), 6.89 (d, J=9.6 Hz, 2H), 4.61 (s, 4H), 4.23 (m, 4H), 4.10 (t, J=6.6 Hz, 4H), 3.89 (m, 4H), 3.71–3.65 (m, 16H), 2.32 (q, J=6.6 Hz, 2H); ^{13}C NMR (CD_3OD) δ 161.23, 159.48, 154.86, 139.32, 133.90, 128.66, 122.08, 74.63, 72.04, 71.96, 71.70, 70.36, 68.00, 52.55, 26.95. MS (FAB, *m/z*) 632 (MH^+, 49). Anal. calcd for $C_{30}H_{41}N_5O_{10}\cdot 3H_2O$: C,52.55; H,6.91; N, 10.21. Found: C, 52.80; H, 6.14; N, 10.22

3.3. Transport rate measurements

The transport experiments were performed at room temperature following a known procedure[11] in a U-tube (9 mm, i.d.). The membrane phase (3 mL of chloroform, Uvasol, Merck), in which the carrier is dissolved (7×10^{-4} mol L^{-1}), lay below and bridged the two aqueous phases. The first aqueous phase (1 mL) contains 5×10^{-5} mol L^{-1} of LiOH, 10^{-1} mol L^{-1} of alkali or ammonium nitrate, and 2×10^{-3} mol L^{-1} of the corresponding alkali or ammonium picrate. The second aqueous phase contains 1 mL of deionized water. The membrane phase is slowly and constantly stirred by a magnetic bar. The picrate concentration in the second aqueous phase, monitored spectroscopically by UV (λ=355 nm), was confirmed to increase linearly with running time (<12 h) and the initial transport rates were calculated. In each case, a similar experiment was carried out in the absence of carrier. The values indicated in Table 3 were estimated from the differences in the transport rates of carrier-containing systems and blank systems (no carrier present). Dibenzo[18]crown-6 was taken as reference ligand, and it showed the following transport rates (μM h^{-1}): Na^+ 22.5; K^+ 198.2; Ca^{2+} 2.4; NH_4^+ 129.0.

3.4. Molecular modelling

Molecular modelling studies were carried out using the AMBER[19] method implemented in the Hyperchem package.[20] When available, the parameters were extracted from the literature.[21] All others were developed following Kollman[22] and Hopfinger[23] procedures. In order to develop suitable parameters for N–H···N hydrogen bonding, ab initio calculations at STO-3G[24] level were used for calculating atomic charges compatible with the AMBER field ones, as Urban et al.[25] claimed that they gave excellent results for the study of ammonium interactions. In all cases, geometries were minimized to a maximun energy gradient of 0.1 kcal/mol using the Polak–Ribiere algorithm, and simulated annealing procedure was used to cover all conformational space running molecular dynamics at 400 K. To optimize host–guests interactions the cation was moved and/or rotated and docked into the cavity of the ligand in all possible positions and then minimized the energy of the complex with no restraints.

Ions are separated far away and well solvated in water. Consequently, there is no need to use counterions.[26] In the absence of explicit solvent molecules, a distance dependent dielectric factor qualitatively simulates the water saturated chloroform environment, as it takes into account the fact that intermolecular electrostatic interactions should die off fast with distance, as the water environment has a high dielectric constant.[27]

Energy of complexation was calculated for each compound, after minimization of the selected trajectory frames, by simulating a complexation process in chloroform saturated with water molecules. It is known that complexes ligand-cation-picrate always include water molecules until solvent saturation is achieved. It has been shown that results obtained in that case follow the same trend that those found from a pure water environment.[15,28] Therefore, the following relation was applied:

$$E_{\text{complexation}} = E_{\text{complex}} - (E_{\text{ammonium}} - E_{\text{ligand}})$$

Acknowledgements

The authors thank the Spanish Comision Interministerial de Ciencia y Tecnologia for the economical support given to this research work (SAF99-0066). We are also grateful to the contribution of the Centro de Resonancia Magnética Nuclear and the Centro de Micro-analisis of the Univ. Complutense.

References and notes

1. Rüdiger, V.; Schneider, H. J.; Solov'ev, V. P.; Kazachenko, V. P.; Raevsky, O. A. *Eur. J. Org. Chem.* **1999**, 1847–1856.
2. Bülhman, P.; Prestch, E.; Bakker, E. *Chem. Rev.* **1998**, *98*, 1593–1687.
3. Strömberg, N.; Hulth, S. *Anal. Chim. Acta* **2002**, *443*, 215–225.
4. Dobler, M. *Comprehensive supramolecular chemistry*; Atwood, J. L., Davies, J. E. D., Mac Nicol, D. D., Vögtle, F., Eds.; Pergamon: Oxford, 1996; Vol. 1, pp 276–313.
5. Lehn, J. M. *Angew. Chem., Int. Ed. Engl.* **1988**, *27*, 89–112.
6. Zhang, X. X.; Bradshaw, J. S.; Izatt, R. M. *Chem. Rev.* **1997**, *97*, 3313–3361.
7. (a) Rodriguez-Franco, M. I.; Navarro, P. *J. Chem. Soc. Chem. Commun.* **1988**, 1365–1367. (b) Navarro, P.; Rodríguez-Franco, M. I. *Trends Org. Chem.* **1993**, *4*, 69–100.
8. Navarro, P.; Pueyo, E.; Rodriguez-Franco, M. I.; Samat, A. *Tetrahedron* **1990**, *46*, 2917–2926.
9. (a) Campayo, L.; Bueno, J. M.; Ochoa, C.; Navarro, P.; Samat, A. *Tetrahedron Lett.* **1993**, *34*, 7299–7300. (b) Campayo, L.;

Bueno, J. M.; Navarro, P.; Ochoa, C.; Jimenez-Barbero, J. M.; Pepe, G.; Samat, A. *J. Org. Chem.* **1997**, *62*, 2684–2693. (c) Reviriego, F.; Navarro, P.; Domenech, A.; Garcia-España, E. *J. Chem. Soc., Perkin Trans. 2* **2002**, 1634–1638.
10. (a) Sanz, A. M.; Navarro, P.; Gomez-Contreras, F.; Pardo, M.; Pepe, G.; Samat, A. *Can. J. Chem.* **1998**, *76*, 1174–1179. (b) Reviriego, F.; Navarro, P.; Domenech, A.; Garcia-España, E. *J. Supramol. Chem.* **2002**, *2*, 115–122.
11. (a) Fierros, M.; Rodriguez-Franco, M. I.; Navarro, P.; Conde, S. *Bioorg. Med. Chem. Lett.* **1994**, *21*, 2523–2526. (b) Rodriguez-Franco, M. I.; Fierros, M.; Martinez, A.; Navarro, P.; Conde, S. *Bioorg. Med. Chem.* **1997**, *5*, 363–367.
12. Druey, J.; Meier, K.; Eichenberger, K. *Helv. Chim. Acta* **1954**, *37*, 121–133.
13. (a) Live, D.; Chan, S. I. *J. Am. Chem. Soc.* **1976**, *98*, 3769–3778. (b) Buchanan, G. W. *Prog. NMR Spectrosc.* **1999**, *34*, 327–377.
14. (a) Lauterbach, M. *J. Phys. Chem. B* **1998**, *102*, 245–256. (b) Troxler, A. L.; Wipff, G. *Anal. Sci.* **1998**, *14*, 43–56.
15. Durand, S.; Dognon, J. P.; Guilbaud, P.; Rabbe, C.; Wipff, G. *J. Chem. Soc., Perkin Trans. 2* **2000**, 705–714.
16. Hobza, P.; Kabelaç Sponer, J.; Mejzlik, P.; Vondrasek, J. *J. Comput. Chem.* **1997**, *18*, 1136–1150.
17. Fyles, T. M. In *Bioorganic chemistry frontiers. Topics in inclusion science*; Osa, T., Atwood, J. L., Eds.; Kluwer Academic, 1991; Vol. 2, pp 59–110 Chapter 2.
18. Morf, W. E.; Ammann, D.; Bissig, R.; Pretsch, E.; Simon, W. *Progress in macrocyclic chemistry*; Izatt, R. M., Christensen, J. J., Eds.; Wiley: New York, 1979; Vol. 1, Chapter 1, pp 2–16.
19. Cornell, W. D.; Cieplak, P.; Bayly, C. I.; Gould, I. R.; Merz, K. M.; Ferguson, D. M.; Spellmeyer, D. C.; Fox, T.; Caldwell, J. W.; Kollman, P. A. *J. Am. Chem. Soc.* **1995**, *117*, 5179–5197.
20. Hyperchem 6.0 (Hypercube Inc.).
21. (a) Fox, T.; Scanlan, T. S.; Kollman, P. A. *J. Am. Chem. Soc.* **1997**, *119*, 11571–11577. (b) Grootenhuis, P. D.; Kollman, P. A. *J. Am. Chem. Soc.* **1989**, *111*, 2152–2158. (c) Moyna, G.; Hernandez, G.; Williams, H. J.; Nachman, R. J.; Scott, A. I. *J. Chem. Inf. Comput. Sci.* **1997**, *37*, 951–956. (d) Boden, C. D. J.; Patenden, G. *J. Comput. -Aided Mol. Des.* **1999**, *13*, 153–166.
22. http://www.amber.ucsf.edu/amber..
23. Hopfinger, A. J.; Pearlstein, R. A. *J. Comput. Chem.* **1984**, *5*, 486–499.
24. Glennon, T. M.; Zheng, Y.-J.; Le Grand, S. M.; Scutzberg, B. A.; Merz, K. M. *J. Comput. Chem.* **1994**, *15*, 1019–1040.
25. Urban, J. J.; Cronin, C. W.; Roberts, R. R.; Famini, G. R. *J. Am. Chem. Soc.* **1997**, *119*, 12292–12299.
26. Wang, J.; Kollman, P. A. *J. Am. Chem. Soc.* **1998**, *120*, 11106–11114.
27. Weiner, S. J.; Kollman, P. A.; Case, D. A.; Singh, U. C.; Ghio, C.; Alagona, G.; Profeta, S.; Weiner, P. *J. Am. Chem. Soc.* **1984**, *106*, 765–784.
28. Hill, S. E.; Feller, D. *Int. J. Mass Spectrom.* **2000**, *201*, 41–58.